pH-induced conformational changes of the Fe^{2+}-N_ϵ(His F8) linkage in deoxyhemoglobin trout IV detected by the Raman active Fe^{2+}-N_ϵ (His F8) stretching mode

Michael Bosenbeck, Reinhard Schweitzer-Stenner, and Wolfgang Dreybrodt
Institute of Experimental Physics, University of Bremen, W-2800 Bremen 33, Germany

ABSTRACT To investigate heme-protein coupling via the Fe^{2+}-N_ϵ(His F8) linkage we have measured the profile of the Raman band due to the Fe^{2+}-N_ϵ (His F8) stretching mode ($\nu_{Fe\text{-}His}$) of deoxyHb-trout IV and deoxyHbA at various pH between 6.0 and 9.0. Our data establish that the band of this mode is composed of five different sublines. In deoxyHb-trout IV, three of these sublines were assigned to distinct conformations of the α-subunit ($\Omega_{\alpha 1}$ = 202 cm^{-1}, $\Omega_{\alpha 2}$ = 211 cm^{-1}, $\Omega_{\alpha 3}$ = 217 cm^{-1}) and the other two to distinct conformations of the β-subunit ($\Omega_{\beta 1}$ = 223 cm^{-1} and $\Omega_{\beta 2}$ = 228 cm^{-1}). Human deoxyHbA exhibits two α-chain sublines at $\Omega_{\alpha 1}$ = 203 cm^{-1}, $\Omega_{\alpha 2}$ = 212 cm^{-1} and two β-chain sublines at $\Omega_{\beta 1}$ = 217 cm^{-1} and $\Omega_{\beta 2}$ = 225 cm^{-1}. These results reveal that each subunit exists in different conformations. The intensities of the $\nu_{Fe\text{-}His}$ sublines in deoxyHb-trout IV exhibit a significant pH dependence, whereas the intensities of the corresponding sublines in the deoxyHbA spectrum are independent on pH. This finding suggests that the structural basis of the Bohr effect is different in deoxyHbA and deoxyHb-trout IV. To analyse the pH dependence of the deoxyHb-trout IV sublines we have applied a titration model describing the intensity of each $\nu_{Fe\text{-}His}$ subline as an incoherent superposition of the intensities from sub-sublines with the same frequency but differing intrinsic intensities due to the different protonation states of the respective subunit. The molar fractions of these protonation states are determined by the corresponding Bohr groups (i.e., $pK_{\alpha 1}$ = $pK_{\alpha 2}$ = 8.5, $pK_{\beta 1}$ = 7.5, $pK_{\beta 2}$ = 7.4) and pH. Hence, the intensities of these sublines reflect the pH dependence of the molar fractions of the involved protonation states. Fitting this model to the pH-dependent line intensities yields a good reproduction of the experimental data. To elucidate the structural basis of the observed results we have employed models proposed by Bangchoroenpaurpong, O., K. T. Schomaker, and P. M. Champion. (1984. *J. Am. Chem. Soc.* 106:5688–5698) and Friedman, J. M., B. F. Campbell, and R. W. Noble. (1990. *Biophys. Chem.* 37:43–59) which describe the coupling between the σ* orbitals of the Fe^{2+}-N_ϵ(His F8) bond and the π* orbitals of the pyrrole nitrogens in terms of the tilt angle Θ between its Fe^{2+}-N_ϵ(His F8)-bond and the heme normal and the azimuthal angle φ between the Fe^{2+}-N_ϵ(His F8) projection on the heme and the N_1-N_3 axis. Our results indicate that each subconformation reflected by different frequencies of the $\nu_{Fe\text{-}His}$-subline is related to different tilt angles Θ, whereas the pH-induced intensity variations of each $\nu_{Fe\text{-}His}$ subline of the deoxyHb trout IV spectrum are caused by changes of the azimuthal angle φ.

INTRODUCTION

The stretching mode of the Fe^{2+}-N_ϵ(His F8) bond between the Fe^{2+} atom of the heme group and the N_ϵ of the proximal histidine (His F8) in the deoxy state of hemoglobin and myoglobin is Raman active and exhibits a low frequency Raman band at $\sim\Omega_{Fe\text{-}His}$ = 220 cm^{-1} (Nagai and Kitagawa, 1980; Nagai et al., 1980). Substantial resonance enhancement of this band is observed upon excitation in the region of the Soret band (Bangcharoenpaurpong et al., 1984).

When deoxyHb changes its quaternary structure from the *R* to the *T* state, the $\nu_{Fe\text{-}His}$ band shifts to higher frequencies. In deoxyHbA within the quaternary *T* state the frequency of the band maximum is at 216 cm^{-1}, whereas the *R* state of the modified deoxy des (Arg141α)Hb-NES exhibits the Raman band at a frequency of 221 cm^{-1} (Nagai et al., 1980).

To correlate the properties of the Fe^{2+}-N_ϵ(His F8)$_2$ bond, monitored by the $\nu_{Fe\text{-}His}$-frequency and the oxygen affinity, Matsukawa et al. (1985) measured the oxygen binding isotherms and the frequencies of the $\nu_{Fe\text{-}His}$-band for a variety of mutant hemoglobins. They observed a definite correlation between the $\nu_{Fe\text{-}His}$ frequency and the first Adair constant K_1, which is related to the free energy of the first oxygenation step. The data revealed an increase of $\Omega_{Fe\text{-}His}$ with decreasing K_1, with variations from 215 cm^{-1} to 225 cm^{-1}. This finding was explained in terms of Perutz's (1970*a*) strain model yielding a theoretical expression which could be fitted closely to the experimental data.

By investigating iron-cobalt-hybrid hemoglobins $\alpha(Fe)_2\beta(Co)_2$ Ondrias et al. (1982) observed the Fe^{2+}-N_ϵ(His F8) stretch frequencies for the individual subunits. For the β-subunit in deoxyHbA $\Omega_{Fe\text{-}His}$ turns out to be 218 cm^{-1} in the *T*-state and 222 cm^{-1} in the *R*-state. The α-subunit exhibits a single band at 220 cm^{-1} in the *R*-state, which is drastically changed upon transition to

Address correspondence to Reinhard Schweitzer-Stenner.

0006-3495/92/01/31/11 $2.00

the *T*-state into a broad band which contains two different sublines at 201 cm^{-1} and 212 cm^{-1}. These two sublines were proposed to arise from a conformational heterogenity of the α-subunits in the *T*-structure.

From these observations one may conclude that even though the $\nu_{Fe\text{-}His}$ line profiles look symmetric, they are composed of several lines due to the α- and β-subunits and conformational heterogenity within these.

The sensitivity of $\Omega_{Fe\text{-}His}$ to structural changes of the protein has been also used to monitor the transient structure on deoxy species within 10 ns after photolysis (Friedman et al., 1983; Friedman, 1985). In the transient state, neither the quaternary *R* nor the tertiary *r* structure of the ligated Hb has been relaxed to the equilibrium structure of the deoxy state. Consequently the $\nu_{Fe\text{-}His}$-band of the transient species is at higher frequency.

All these experiments show that the Fe^{2+}-N_ϵ(His F8)-stretching mode is particularly suited to monitor changes in the tertiary as well as in the quaternary structure. A wide variety of experimental data has therefore been accumulated which are comprehensively reviewed by Kitagawa (1988) and Friedman and Rosseau (1988).

The $\nu_{Fe\text{-}His}$-band also exhibits variations of its intensity upon structural changes in the apoprotein. This has been established by means of cyrogenic studies of myoglobin by Sassaroli et al. (1986). They have measured the intensity and the frequency of the $\nu_{Fe\text{-}His}$-band of transient species at different temperatures between 4*K* and 77*k*. Their results reveal that the intensity of the transient $\nu_{Fe\text{-}His}$ band increases with increasing temperature. Its frequency, however, does not exhibit any change.

To explain the properties of the Fe^{2+}-N_ϵ(His F8) stretching vibration Sassaroli et al. (1986) applied a coupling model proposed by Bangcharoenpaurpong et al. (1984). These authors suggested that the coupling between the σ* orbital of the Fe^{2+}-N_ϵ-bond and the π* orbital of the pyrrole nitrogens depends critically on the position of the Fe-N_ϵ-axis with respect to the heme plane. Two angles define this position, namely the polar tilt angle Θ between the Fe^{2+}-N_ϵ-bond and the normal of the heme plane and the azimuthal angle φ between the projection of the Fe^{2+}-N_ϵ-axis on the heme plane and the N_1-Fe^{2+}-N_3 axis (cf Fig. 5). The σ*-π*-overlap increases with increasing Θ and decreasing φ. If this coupling results in significant transfer of electron density to the porphyrin π-system, the frequency of the $\nu_{Fe\text{-}His}$-mode will be affected. This, however, need not necessarily be the case and it is also possible that changes of intensity occur without any frequency shift of the line, in accordance with the results emerging from the cyrogenic studies (Sassaroli et al., 1986). Recently Friedman et al. (1990) provide further experimental evidence that the intensity of the $\nu_{Fe\text{-}His}$-band is mainly determined by the azimuthal angle φ whereas the frequency depends on the tilt angle Θ.

Hence, due to the coupling scheme of Bangcharoenpaurpong et al. (1984) and Friedman et al. (1990) the $\nu_{Fe\text{-}His}$ line may change in frequency and intensity upon external perturbations of the protein affecting the heme moiety. Such perturbations do also result from changes of pH in the solution. These lead to binding or release of protons at allosteric Bohr groups influencing oxygen affinity (Bohr effect, Perutz, 1970*b*). It has been shown in a series of papers from our group, reviewed by Schweitzer-Stenner. (1989), that one can investigate these changes by means of resonance Raman spectroscopy. The depolarization ratio dispersion of the ν_4-electron-density-marker line and the ν_{10}-core-size-marker line of ligated hemoglobin A, for instance, are both sensitive to pH. From a theoretical analysis of these data, one finds that upon protonation of allosteric amino acid residues distortions of the heme are induced, which affect its oxygen binding properties (Schweitzer-Stenner et al., 1986, 1989*a*, *b*). These pH-induced distortions might be also reflected in a pH-dependence of the $\nu_{Fe\text{-}His}$ line profiles. Therefore, the first part of this study deals with the pH dependence of the line profile of the $\nu_{Fe\text{-}His}$-band of deoxyHb-trout IV. This molecule exists in the quaternary *T*-state with all its subunits in the tertiary *t*-state at pH between 5–9. By means of a thorough analysis of the oxygen binding isotherms of Hb-trout IV carried out in terms of an extended Herzfeld-Stanley model (Herzfeld and Stanley, 1974; Schweitzer-Stenner and Dreybrodt [1989]) have shown that each of the subunits locates two Bohr groups with almost equal pK values. For the *t*-state these are $pK_{\alpha 1} = pK_{\alpha 2} = 8.5$ in the α-chains, and $pK_{\beta 1} = 7.5$ and $pK_{\beta 2} = 7.4$ in the β-chains.

The first part of this study is aimed to elaborate the influence of the protonation of these Bohr groups on the heme-protein linkage as monitored by the $\nu_{Fe\text{-}His}$ band. In the second part of the paper, we reinvestigate the $\nu_{Fe\text{-}His}$ bands of deoxyHbA. Comparison with the results on deoxyHb-trout IV reveals that the mechanism of the Bohr effect is different for human and trout Hb.

MATERIAL AND METHODS

Preparation of hemoglobin

Trout hemoglobin (Salmo irideus) was prepared according to the procedure described by Schweitzer-Stenner et al. (1989*a*). Hemoglobin A was prepared by employing standard procedures (Spiro and Strekas, 1974). Dialyzing the samples against 0.1 M Tris-HCL-buffer (pH > 7.0) or bis-tris-HCL-buffer(pH < 7.0) different pH-values could

be adjusted. The concentration of each sample was 650 μM as determined by measuring the absorbance with a HP-diode-array spectrometer. By adding a few grains of sodium dithionite, each sample attained the deoxy state. To avoid oxygenation anaerobic conditions were maintained during the experiment. The temperature of the sample was kept at 4°C.

Measurement of the Raman spectra

The low frequency spectra of deoxyHb-trout IV and deoxyHbA were obtained using the 457.9 nm line of an Argon-ion laser at an average power of 300 mW. The Raman radiation was measured in the backscattering configuration. The laser beam, polarized perpendicular to the scattering plane, was focussed by a cylindrical lens of 10 cm focal length onto the sample cuvette which was situated in a copper block for cooling (T = 6°C). In comparison with experiment using a spherical lense in a rectangular scattering geometry the power density in the focus is thus reduced by a factor of ~50. The scattered light was dispersed by a Spex 1401 monochromator (SPEX Inds. Inc., Edison, NJ) with a spectral resolution of 2 cm^{-1}. In each measurement the time for recording the spectrum did not exceed 2 min. To check the ligation/oxidation state of the chromophore, the high frequency part of the Raman spectrum was detected at each pH after measuring the band profile of the $\nu_{Fe\text{-}His}$ mode. No contamination of the sample by oxy-or methemoglobin was observed. The scattered photons were detected by a cooled photomultiplier (model 31034, RCA, Lancaster, PA) and registrated by a photocounting system (Ortec). The data were digitized and transferred to an AT personal computer (Confident, Taiwan) for storing and further analyzation.

Analysis of the line profile

The line profile of the $\nu_{Fe\text{-}His}$-band was analyzed by means of a computer program substracting the background and decomposing the profile alternatively into Lorentzian or Gaussian sublines with different frequencies and halfwidths. To identify the frequencies and the halfwidths of the sublines contributing to the observed band we have computed the second derivative of the smoothed line profiles (Perkampus, 1986). The frequency values were determined by use of the plasma line at 460.96 nm which appeared in the Raman spectra at 143 cm^{-1} (cf Fig. 1). The statistical error of the derived frequency values was estimated to ±1 cm^{-1}. The intensity of the sublines was derived by means of the following procedure: First we describe the band profile as a superposition of i sublines using:

$$I_\Omega = \sum_i A_i P_i(\Omega_i - \Omega), \quad (1)$$

where I_Ω is the band intensity at frequency Ω, P_i is the normalized profile of the iTH subline at frequency Ω_i and A_i denotes the corresponding amplitude.

To calculate the amplitudes A_i we consider the intensity $I_{\Omega j}$ at the frequency Ω_j of a distinct subline j, which is given by:

$$I_{\Omega j} = \sum_i A_i P_i(\Omega_i - \Omega_j) \quad (2)$$

where $i = 1,2,..,j,..N$ (N: number of sublines).

Eq. 2 can be formulated for all frequencies Ω_i. Thus one obtains a set of inhomogeneous linear equations, which can be solved by use of a Gaussian algorithmus to calculate the amplitudes A_i.

The total intensity I_i of the iTH subline can now be calculated using:

$$I_i = A_i \Gamma_i F(P_i) \quad (3)$$

where Γ_i denotes the halfwidth of the iTH subline. The factor $F(P_i)$ depends on the choice of the profile.

By fitting Eq. 2 to the data slight variations of the frequency ($\delta\Omega = \pm 1$ cm^{-1}) and the halfwidth ($\delta\Gamma = \pm 0.5$ cm^{-1}) were allowed for fine tuning. By measuring samples from different preparations for several times the spectra could be reproduced with an accuracy of 10%.

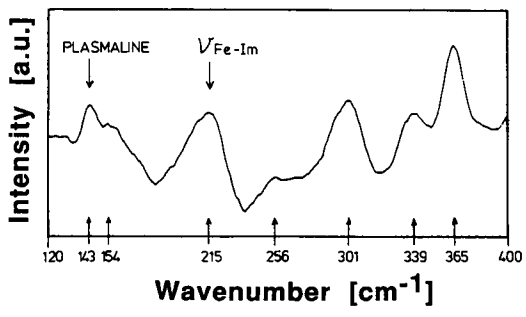

FIGURE 1 (a) Resonance Raman spectrum of deoxyHb-trout IV between 120 cm^{-1} and 400 cm^{-1} excited by the 457.9-nm line of an Argon-ion laser. Experimental parameters: heme concentration 650 μM, pH = 6.1, T = 4°C, spectral resolution ≈ 2 cm^{-1}.

RESULTS

Raman data of hemoglobin trout IV

The Raman spectra in the low frequency region (100 cm^{-1} – 400 cm^{-1}) of deoxyHb-trout IV were recorded at twelve different pH-values between 6.0 and 9.0. The spectrum detected at pH = 7.4 is shown in Fig. 1. Apart from other intensive resonance Raman bands arising from porphyrin ring vibrations the mode of interest is located between 200 cm^{-1} and 230 cm^{-1}. The spectrum was remeasured several times under the same experimental conditions. Thereafter this protocol was repeated using another two preparations. Furthermore we repeated the measurement on the sample adjusted to pH = 8.4 using a reduced power of the incident laser beam (160, 80, 50, and 12 mW). In all cases we find identical line shapes.

Fig. 2 shows three smoothed line profiles of the $\nu_{Fe\text{-}His}$ line measured at pH = 6.1, 7.5, and 8.4. These data reveal that the line shape depends on pH. The maximum is shifted from 222 cm^{-1} at pH = 8.4 to 216 cm^{-1} at pH = 6.1. The asymmetric shape of the three profiles clearly indicates that the $\nu_{Fe\text{-}His}$ band is composed of different sublines. These can be identified by computing the second derivative of the band profile (cf Materials and Methods). This procedure reveals the existence of five different sublines the frequencies of which are 202 cm^{-1},

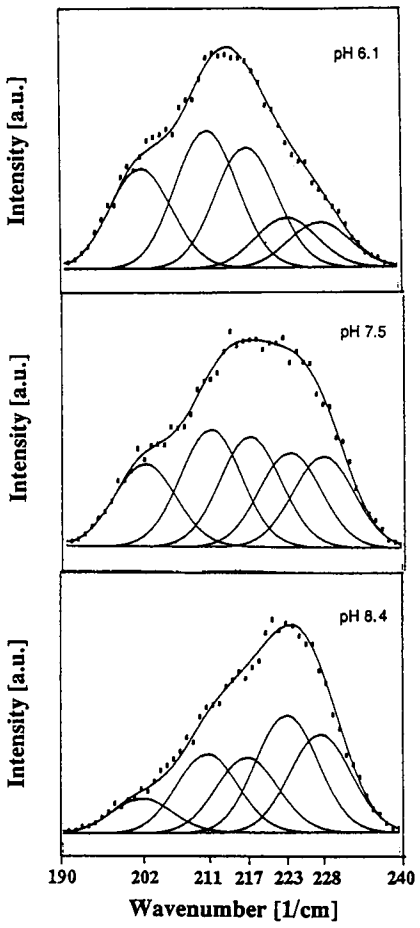

FIGURE 2 Line profiles of the $\nu_{Fe\text{-}His}$-band of deoxyHb-trout IV measured at pH = 6.1, 7.5, and 8.4. Each profile was decomposed into five distinct Gaussian sublines with frequencies 202 cm^{-1}, 211 cm^{-1}, 217 cm^{-1}, 223 cm^{-1}, and 228 cm^{-1} as displayed in the diagrams. The halfwidth of each subline is 12 cm^{-1}.

211 cm^{-1}, 217 cm^{-1}, 223 cm^{-1}, and 228 cm^{-1} as shown in Fig. 3 for pH = 7.5. The frequencies of these five lines and their halfwidths (12 cm^{-1}) turned out to be identical within the limit of accurracy (1 cm^{-1} for the frequencies and 0.5 cm^{-1} for the halfwidths) at all pH-values between 6 and 9, i.e., a total of twelve distinct band profiles.

The intensities of the sublines were calculated using Gaussian profiles in Eqs. 2 and 3. They exhibit a significant dependence on pH as displayed in Fig. 4. The low frequency sublines at 202 cm^{-1}, 211 cm^{-1} and 217 cm^{-1} show decreasing intensities upon increasing pH. The high frequency sublines at 223 cm^{-1} and 228 cm^{-1} exhibit increasing intensities with rising pH. The solid lines result from a fit discussed in the next section.

All band profiles could be fitted also by means of

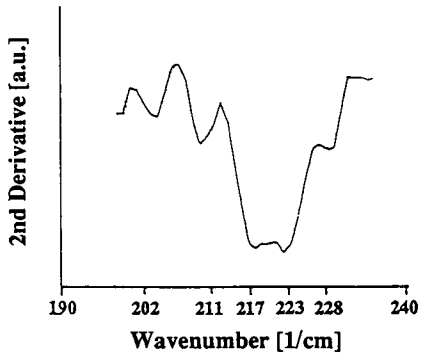

FIGURE 3 Second derivative of the band profile due to the $\nu_{Fe\text{-}His}$-mode of deoxyHb trout IV measured at pH = 7.5. The minima indicate the frequency positions of the sublines.

Lorentzian line profiles. The thus obtained titration curves are practically identical to those derived from the analysis with Gaussian line profiles.

One may raise the question whether the number of sublines composing the $\nu_{Fe\text{-}His}$-band can be reduced by increasing the halfwidths of the corresponding Gaussian profiles. In fact, it can be shown that some bands,

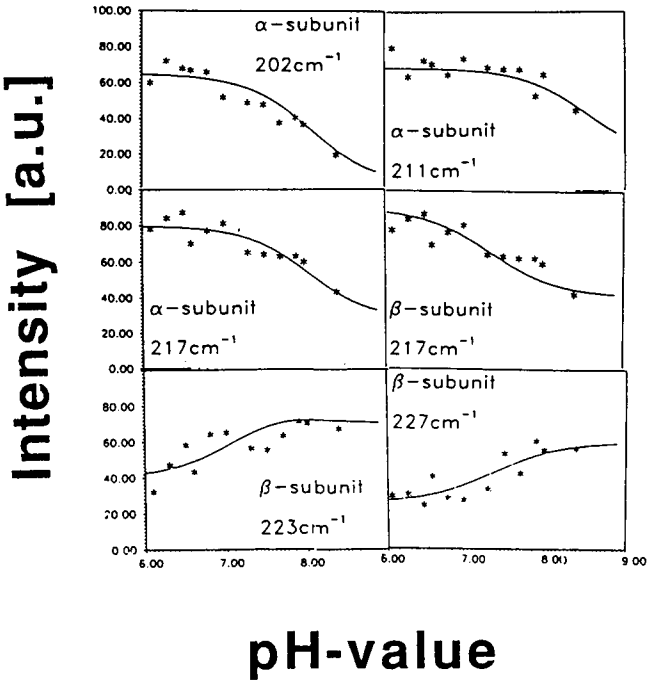

FIGURE 4 pH-dependence of the intensity of the five Raman sublines contributing to the $\nu_{Fe\text{-}His}$-band of deoxyHb-trout IV. The frequencies and the assigned subunit are indicated in the respective diagrams. The full lines result from the fits of the data to model II.

especially those measured at pH = 6.0 and pH = 8.0, can be fitted in terms of a reduced number of sublines. It turns out, however, that with a number of four instead of five sublines it is not possible to fit all $\nu_{Fe\text{-}His}$-band profiles measured at twelve pH-values between 6.0 and 9.0.

Analysis of the pH-dependence of the deoxyHb-trout IV Fe^{2+}-His(F8) lines

The analysis of the titration curves shown in Fig. 4 requires knowledge about the quaternary and tertiary state of deoxyHbA. From the analysis of the oxygen binding isotherms of Hb-trout IV (Brunori et al., 1978) it turns out that the fully deoxygenated molecule is in the quaternary *T*-state with all its subunits in the tertiary *t*-state independent on pH (Schweitzer-Stenner and Dreybrodt, 1989). These data set, however, does not cover the pH-region >pH = 8.0. Therefore, one may argue that a $T \rightarrow R$ transition of the deoxygenated molecule occurs at alkaline pH as obtained for deoxyHb-carp (Noble et al., 1970; Chien et al., 1980). Earlier measurements of both, the Hill coefficient and the allosteric equilibrium constant L_0 of Hb trout IV rule out this possibility (cf Brunori et al., 1975). Only a small increase of the Hill coefficient and a small reduction of L_0 at pH > 8.0 were found. At pH = 8.5 L_0 still exhibits a value of 10^2. Hence, we conclude that in our experiments the deoxygenated Hb remains in the quaternary *T*-state even at pH > 8.0.

From the fit to the O_2 binding curves the authors obtained two Bohr groups in each subunit. The respective pK values are 8.5 for the two amino acid residues in the α-chains, and 7.5/7.4 for the two groups in the β-subunits. The assignment of the pK values to the subunits was made by considering structural aspects of the Root effect reported by Perutz and Brunori (1982). According to the occupation number $i,j = 0, 1$ of the two Bohr groups each subunit *S* can exist in four different titration states C^{ij}s.

The first model (model I) applied to explain the pH dependence of the subline's intensities was based on the following assumptions: (*a*) the sublines are related to distinct conformational substates of the Fe^{2+}-His(F8)-linkage in one particular subunit; (*b*) thermodynamic equilibrium exists between the different conformational substates of each subunit; (*c*) the protonation of the Bohr groups affects the equilibrium between these substates, thus changing the apparent intensity of the sublines; (*d*) the intensity of each subline is proportional to its molar fraction.

Assuming, as an example, only two conformational substates with one Bohrgroup in each subunit *S*, this model can be illustrated by the following scheme:

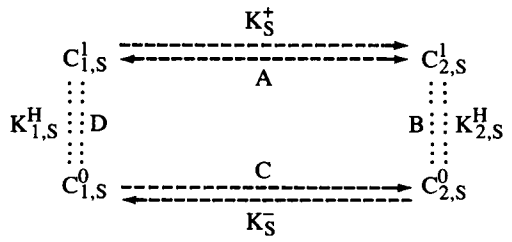

Reaction *A* denotes the transition among the two conformations $C^1_{1,s}$ and $C^1_{2,s}$ where the allosteric site is protonated. Reaction *C* is the corresponding transition between the deprotonated conformations $C^0_{1,s}$ and $C^0_{2,s}$. Reactions *B* and *D* represent the protonation of the Bohr group in conformations 1 and 2, respectively. Due to assumption (*c*) $K^+_{1,s}$ is different from $K^-_{2,s}$. This implies that due to free energy conservation the pK value of the Bohr group undergoes a shift upon the $1 \rightarrow 2$ transition of the corresponding subunit.

In our case we have to consider two Bohr groups and a set of *m* subconformations per subunit *S* which is still to be determined. The apparent intensities $I_{m,s}$ of the respective sublines can be calculated in dependence of pH using the equation:

$$I_{m,s}(\mathrm{pH}) = \sum_{ij} X^{ij}_{m,s}(\mathrm{pH}, K^H_{1,s}, K^H_{2,s}, K_s^-)\, I_{m,s} \qquad (4)$$

where $X^{ij}_{m,s}$ is the molar fraction of the *m*TH conformation existing in the protonation state C^{ij}_s ($i,j = 0, 1$ label the occupation of the two Bohr groups). Its calculation is given in Appendix A1. $I_{m,s}$ denotes the intrinsic intensity of the $\nu_{Fe\text{-}His}$ subline in the *m*TH subconformation of subunit *S* which would be observed if its molar fraction would be equal to one.

When fitting this model to the data we used the constants $K^{ij}_{mm'}$, related to the equilibrium between the conformations *m* and m' in the protonation state C^{ij}_s and the intrinsic intensities $I_{m,s}$ as free parameters. As pK values of a distinct subconformation *m* we used the *t*-state pK values of the Bohr groups reported by Schweitzer-Stenner and Dreybrodt (1989) (i.e., $pK_{\alpha 1} = pK_{\alpha 2} = 8.5$; $pK_{\beta 1} = 7.5$, $pK_{\beta 2} = 7.4$). The pK shifts were derived from the obtained $K^{ij}_{mm',s}$ values by use of the law of free energy conservation. Because we do not have any a priori knowledge on the assignment of the five sublines derived from the band profiles to the α and β-subunits, we used alternatively both sets of pK values in fits to various combinations of the titration curves of the sublines.

Fitting our data to this model clearly shows that reproduction of the data requires drastic shifts of the pK values of the Bohr groups upon the transition between different subconformations (pK = 1.0–1.5). This is an

unreasonable result. Furthermore, in most of the attempts, the data were not fitted in a satisfactory way. These findings suggest that the pH-dependence of the subline's intensities is not predominantly caused by pH-induced changes of the equilibrium between the conformational substates.

In a second attempt to describe our data we used an alternative model (model II) based on the following assumptions: (*a*) protonation of the Bohr groups does not change the equilibrium between the different subconformations giving rise to the distinct sublines. Thus, the equilibrium constants $K^{ij}_{mm',s}$ are independent on the protonation state of the corresponding subunit *s* and no pK shift occurs upon the $m \rightarrow m'$ transition; (*b*) the intrinsic intensity of each Raman line in a distinct subconformation depends on its protonation state, whereas its frequency and halfwidth is unaltered upon protonation.

The apparent intensity $I_{m,s}$ of the subline i_m of a subconformation *m* can then be regarded as an incoherent superposition of the corresponding four different sub-sublines where each protonation state exhibits differing intrinsic intensities $I^{ij}_{m,s}$. It is therefore determined by the molar fractions of the four titration states C^{ij}_s with reactions due to the following scheme:

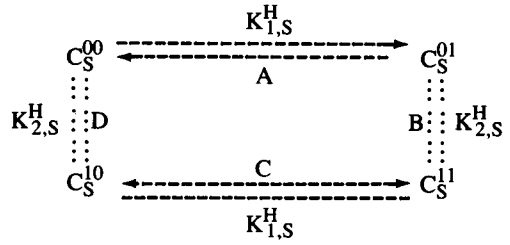

$K^H_{1/2,s} = -RT\ pk_{s1/2}$ are the proton binding constants of the two Bohr groups. The reactions are: (*a*) (protonation of Bohr group 1 in subunit *S*), (*b*) (protonation of Bohr group 2, when group 1 is already protonated), (*c*) (protonation of Bohr group 2) and (*d*) (protonation of Bohr group 1, when group 2 is already protonated).

The pH-dependent total intensity of each subline is then written as:

$$I_{m,s} = \sum_{ij} \tilde{X}^{ij}_s(\mathrm{pH})\, X_{m,s}\, I^{ij}_{m,s} \qquad (5)$$

where $X_{m,s}$ is the molar fraction of molecules in the conformation m. $\tilde{X}^{ij}_s(\mathrm{pH}) = X^{ij}_s / X_{m,s}$ is the molar fraction of the titration state C^{ij}_s with respect to a distinct conformation m of the subunit *S*. Its calculation is given in Appendix A2.

By fitting the data to this model we allowed the unknown products of molar fraction and corresponding intrinsic intensities $X_{m,s} I^{ij}_{m,s}$ as parameters. The molar fractions $\tilde{X}^{ij}_s(\mathrm{pH})$ were calculated by inserting the *t*-state pK values of the Bohr groups reported by Schweitzer-Stenner and Dreybrodt (1989) into Eq. (A2.1).

Each of the curves shown in Fig. 4 was fitted to the data due to the following protocol. First we used the pK values assigned to the α chain to fit the titration curves of all sublines. It turned out that only the data of the lines at 202 cm^{-1}, 211 cm^{-1} and 217 cm^{-1} could be reproduced. In a second step, we employed the pK values assigned to the β subunit in a fit to all diagrams in Fig. 4. By this procedure the titration curves of the lines at 217 cm^{-1}, 223 cm^{-1} and 228 cm^{-1} were reproduced. The fits to the data of the lines at 202 cm^{-1} and 211 cm^{-1}, however, were not convincing. The successful fits are represented by the full lines in Fig. 4. These findings suggest, that both subunits exhibit at least two conformations monitored by the Raman sublines $\nu_{\text{Fe-His},\alpha 1}$ ($\Omega_{\alpha 1}$ = 202 cm^{-1}) and $\nu_{\text{Fe-His},\alpha 2}$ (Ω_2 = 211 cm^{-1}) for the α chains and by the sublines $\nu_{\text{Fe-His},\beta 1}$ ($\Omega_{\beta 1}$ = 223 cm^{-1}) and $\nu_{\text{Fe-His},\beta 2}$ ($\Omega_{\beta 2}$ = 228 cm^{-1}) for the β chains, respectively. The data do not allow an unambigious assignment of the subline at 217 cm^{-1} which is well represented in both fits.

The mole fractions $\tilde{X}^{ij}_s(\mathrm{pH})$ of the titration states of the α and β subunits are shown in Fig. 5. Because in both subunits pK_{s1} is nearly equal to pK_{s2}, the mole fractions of the protonation states [1, 0] and [0, 1] are almost identical at all pH. As a consequence the fitting procedure does not yield the fitting parameters $I^{10}_{m,s} X_{m,s}$ and $I^{01}_{m,s} X_{m,s}$ independently. Instead, only the sum of the two parameters can be obtained. Table 1 lists the parameter values emerging from the fitting procedure.

The data give evidence that a dramatic change of intrinsic Raman intensity can result by deprotonation.

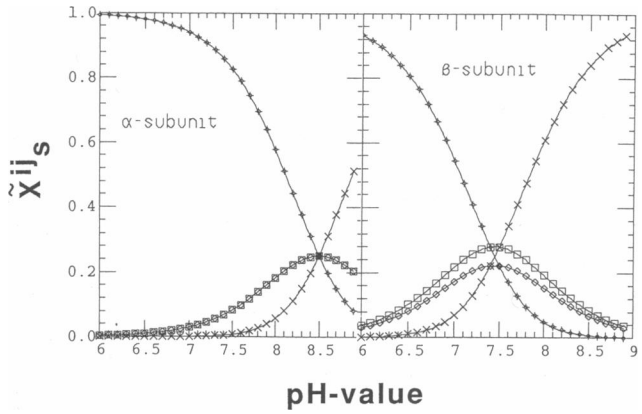

FIGURE 5 pH-dependence of the molar fractions $X^{ij}_{m,\alpha}$ and $X^{ij}_{m,\beta}$ of the titration states (*i*, *j*) exhibited by deoxyHb-Trout IV. The respective titration states are labeled by the following symbols: □: [0, 0], ◇: [0.1], △: [1, 0], ×: [1, 1].

TABLE 1 **Values of the parameters obtained from the fits to the titration curves shown in Fig. 4**

Protonation state	$I^{ij}_{m,s}X_{m,s}$		
$[i,j]$	α(1), 202cm^{-1}	α(2), 211cm^{-1}	α(3), 217cm^{-1}
[1,1]	65	69	80
[0,1] + [1,0]	20	100	60
[0.0]	6	15	30
Protonation state	$I^{ij}_{m,s}X_{m,s}$		
$[i,j]$	β(1), 217cm^{-1}	β(2), 223cm^{-1}	β(3), 227cm^{-1}
[1,1]	90	70	25
[0,1] + [1,0]	120	160	92
[0.0]	42	40	60

Units are arbitrary.

This is especially true for the conformation $C_{\alpha(1)}$, where the intensity drops by a factor of ten upon complete deprotonation.

In summary, we state that model 2 provides an appropriate description of our data, although it might not be excluded that small contributions via the process described by model 1 are also present.

Raman data of deoxyHb

To compare our results on deoxyHb trout IV with the properties of the $\nu_{Fe\text{-}His}$ band of a more elaborated heme protein, we have measured the line profile of the corresponding deoxyHbA band at various pH between 6.0 and 9.0. As shown in Fig. 6 this band can be decomposed into four different Gaussian sublines. From the second derivative of the smoothed band shapes one derives the frequencies 203 cm^{-1}, 212 cm^{-1}, 220 cm^{-1} and 227 cm^{-1} with a common halfwidth of 12 cm^{-1}. In the limit of accuracy, the intensities of these sublines do not depend on pH. An assignment of the sublines is proposed in the discussion.

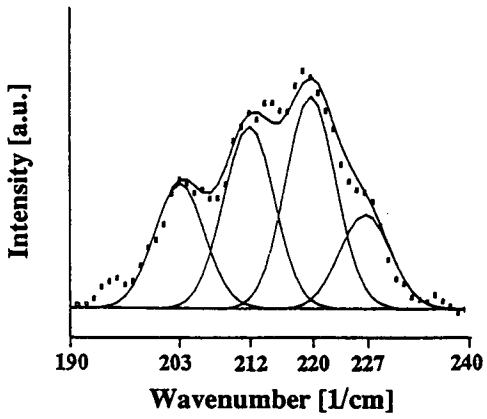

FIGURE 6 Line profile of the $\nu_{Fe\text{-}His}$-band of deoxyHbA measured at pH = 6.4. The profile was decomposed into four distinct sublines with frequencies 203 cm^{-1}, 212 cm^{-1}, 220 cm^{-1}, and 227 cm^{-1} as displayed in the diagram.

DISCUSSION

Coupling model to explain the pH-induced intensity variations of the Fe^{2+}-His(F8) sublines

To account for the resonance Raman enhancement of the $\nu_{Fe\text{-}His}$ band in the region of the *B*-absorption band Bangcharoenpaurpong et al. (1984) proposed a model describing the coupling between the wave functions of the Fe^{2+}-N_ϵ σ*-bond and the π* orbitals of the pyrrole nitrogen atoms. The geometry of the Fe^{2+}-N_ϵ(His F8) bond is shown in Fig. 7. The direction of the Fe^{2+}-N_ϵ axis is specified by the polar angle Θ and the azimuthal angle ϕ as shown in *a*). Θ is in the order of 10° and decreases to zero upon ligand binding. The azimuthal angle ϕ ranges from 15–25° in the deoxy structure and is also reduced by ligand binding (Baldwin and Chothia, 1979). The overlap of the antibonding σ* orbital with the π* orbital depends on these angles. It increases with increasing Θ. In dependence on the azimuthal angle ϕ, it shows a maximum at ϕ = 0 and decreases with increasing angle. Therefore the mixing of the *B* band orbitals into the wavefunctions σ*, which locates one electron, gives rise to resonance enhancement in the *B* band. There is also an effect to the mode frequency via changes in the electron–electron repulsion of the σ* electrons with the bonding π orbitals at the pyrrole nitrogen N_3. Therefore reduction in ϕ should cause an increase of the mode frequency. Similarly, an increase in the polar angle should reduce the mode frequency. Thus, in the ligated *r*-state, where Θ and ϕ are both reduced drastically (Baldwin and Chothia, 1979, Shaanan, 1983) one expects a significant decrease of the intensity and a frequency shift of the Raman band towards higher energies. This might be the reason why it has not yet been observed.

Even though the model of Bangcharoenpaurpong et al. (1984) accounts for many properties of the $\nu_{Fe\text{-}His}$-line (for instance, the excitation profiles in the B-band region), it has implications which are not consistent with some experimental results. This mainly concerns the close relationship between frequency and intensity. Whereas the temperature dependence of the $\nu_{Fe\text{-}His}$ from the photoproduct of myoglobin-CO shows an increase in intensity with rising temperature between 2–200 *K*, a corresponding frequency shift of the band was not observed (Sassaroli et al., 1986). More recently Friedman et al. (1990) reported resonance Raman spectra from a deep ocean fish hemoglobin *Coryphaenoides*

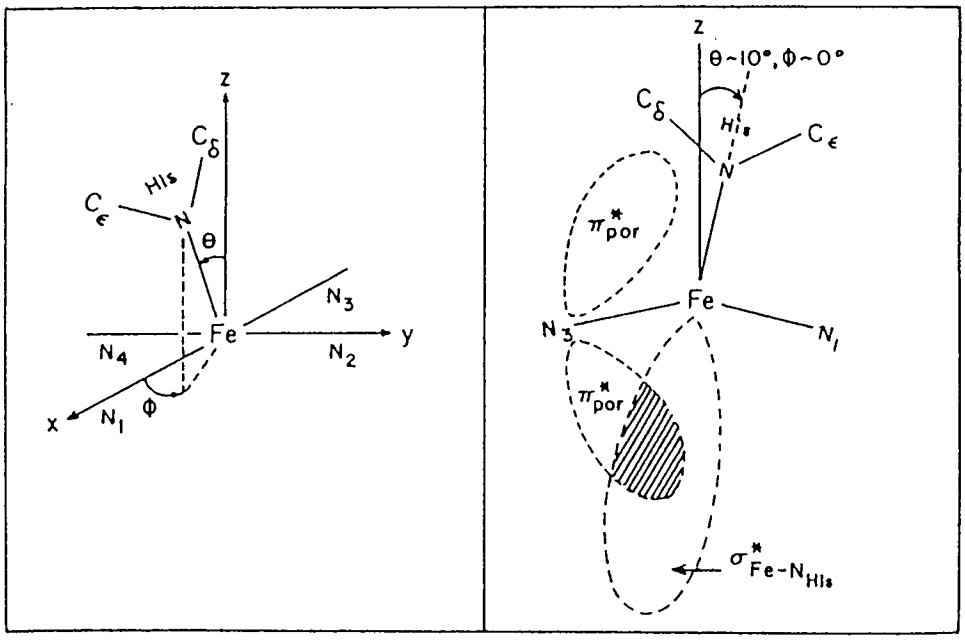

FIGURE 7 Schematic representation of the model describing the coupling between the σ*-orbital of the Fe-His(F9)-bond and the π* orbitals of the pyrrole nitrogen atoms. The position of the Fe^{2+}-N_ϵ(His F8)-bond with respect to the heme is determined by the polar angle Θ and the azimuthal angle ϕ (from Bangcharoenpaurpong et al., 1984).

armatus (Hb c.a.) exhibiting a $\nu_{Fe\text{-}His}$-band which is more intensive by a factor of three than the corresponding band in the deoxyHbA-spectrum whereas their apparent frequency is nearly identical to that in deoxyHbA.

To account for these experimental findings Friedman et al. (1990) proposed a modified version of the coupling model suggested by Bangcharoenpaurpong et al. (1984). They assumed that the mode frequency is predominantly controlled by the polar angle Θ, whereas its intensity is mainly determined by the azimuthal angle ϕ overlap. This coupling model is corroborated by extended Hückel calculations of Scheidt and Chipman (1986). They showed that for five coordinated iron porhyrins in solution the experimentally observed azimuthal angles ϕ can be explained as resulting from a balance between nonbonded steric interactions (favoring a large ϕ) and π-interactions between the Pπ orbitals of the iron and the imidazole nitrogen (N_ϵ) (favoring a more eclipsed conformation with small angles ϕ). The Fe^{2+}-N_ϵ(His F8) bond is predominantly of σ-character. Thus, one expects that it is not significantly affected by variations in the azimuthal angle ϕ.

The ligand affinity of the central Fe^{2+} atom is controlled by both angles of the $Fe^{2+}N_\epsilon$(His F8) bond. As shown by Friedman (1985) an increase of the polar angle Θ (monitored by the decreasing apparent frequency of the $\nu_{Fe\text{-}His}$ band) enhances the repulsive interaction between the imidazole and a pyrrole nitrogen (N_p) thus lowering the geminate recombination of photolyzed ligands. Consequently one expects that diminishing the azimuthal angle ϕ also yields an enlarged energy barrier for ligand binding. This is in accordance with the results on deoxyHb(c.a.) which exhibits an extremely low affinity of its tertiary *t*-state and a very intensive $\nu_{Fe\text{-}His}$-band indicating to a eclipsed position of the proximal imidazole. Our Raman data on the $\nu_{Fe\text{-}His}$ mode of deoxy trout IV clearly support the model of Friedman et al. (1990) because it shows that variations in intensity are not coupled to variations in frequency. We therefore conclude that the protonation of Bohr groups causes changes of the azimuthal angle ϕ rather than affecting the polar angle Θ. Thus the intensity of each sub-subline contributing to a distinct subline of the $\nu_{Fe\text{-}His}$-band of deoxyHb trout IV is determined by its azimuthal angle ϕ, which is different in each protonation state of a given subconformation. The different sublines of the $\nu_{Fe\text{-}His}$ band, however, result from different tilt angles Θ in each corresponding subconformation. Hence, by use of the coupling model of Friedman et al (1990) the following conclusions can be drawn from the Raman data on deoxyHb trout IV: (*a*) The Fe^{2+}-N_ϵ(His F8) bond of the α subunits exhibits larger polar angles Θ than that of the β subunits. This indicates that the heme protein coupling at the Fe^{2+}-N_ϵ(His F8)-linkage is stronger in the α- than in the β-subunits. This is in accordance with what has been found for deoxyHbA by investigating iron-cobalt hybrid

hemoglobin (Ondrias et al., 1982). (*b*) The protonation of Bohr groups in the α subunit increases the intensity of the corresponding sublines (i.e., $\Omega_{\alpha 1} = 202$ cm^{-1}, $\Omega_{\alpha 2} = 211$ cm^{-1}, probably also $\Omega_{\alpha 3} = 217$ cm^{-1}; cf Fig. 4) indicating to a decrease of the azimuthal angle ϕ and an enhanced distortion of the heme by repulsive N_ϵ(His(F8))-N_p-interactions. Thus the protonation of the Bohr groups in the α-subunits effect a heme conformation the ligand affinity of which is most probably reduced compared with the deprotonated state. (*c*) In the β-subunits the protonation of the Bohr groups cause a reduction of the heme-His(F9)-interaction as reflected by the decrease of the intensity of the corresponding sublines with lowered pH (Fig. 4). Thus one would expect that the apparent intrinsic affinity of the β-subunits increases rather than decreases towards acid pH. (*d*) The parameters $I^{ij}_{s(v)}X_{s(v)}$ listed in Table 1 indicate that especially in the β-subunits the protonation of the Bohr groups may counteract each other. The protonation of one of the Bohr groups lowers ϕ (increasing intensity of the sublines) whereas it is raised by the protonation of the second group (decreasing intensity of the subline).

Comparison between deoxyHbA and deoxyHb trout IV

Whereas the Fe-His-band of deoxy Hb trout IV exhibits a significant dependence of pH between pH = 6.0 and 9.0, the corresponding band-profile of deoxyHbA is pH independent. Hence, our results indicate that the mechanism of the alkaline Bohr effect is quite different in HbA and Hb-trout IV. This is in close agreement with other Raman data. Schweitzer-Stenner et al. (1984) measured the depolarization ratio dispersion for resonance Raman scattering of the ν_4-oxidationmarker line (1,355 cm^{-1}) of the deoxyHbA spectrum, thus monitoring symmetry lowering distortions of the heme by protonation of allosteric groups.

Although a drastic pH dependence occurs below pH = 6.0, no changes are observed for pH in the physiological region. This shows that protonation of Bohr groups (i.e., $pK_\alpha = 8.2$; $pK_{\beta 1} = 7.8$, $pK_{\beta 2} = 7.1$; Kilmartin et al., 1980; Schweitzer-Stenner et al., 1989*b*) does not influence the heme symmetry. In contrast to this, the ν_4-line of deoxyHb-trout IV shows a marked pH dependence of its depolarization ratio dispersion in the pH-region between 6.0 and 9.0, which was explained in terms of the very same pK values used to rationalize the intensity variations of its Fe^{2+}-His(F8) sublines (Bosenbeck, 1990). A detailed discussion of this observation will be given in a future paper (Bosenbeck et al., manuscript in preparation).

The assignments of the sublines of deoxyHbA can be made by use of Raman data obtained by Ondrias et al. (1982). To explore the contributions of the α and β subunits to the band profiles of the Fe^{2+}-His(F8)-mode in deoxyHbA the authors have investigated iron-cobalt hybrid hemoglobins, namely $\alpha(Fe)_2\beta(CO)$ and $\alpha(Co)_2\beta(Fe)_2$ of HbA and des(Arg(141α))-HbA. The latter molecule is known to exist in the quaternary *R*-state. Due to their analysis of the data the $\nu_{Fe\text{-}His}$ frequency for the β subunit occurs at 218 cm^{-1} and 222 cm^{-1} for the HbA (*T*-state) des(Arg(141α))-HbA (*R*-state) (*R*-state) respectively. For the α-subunits, the Fe^{2+}-His(F8)-frequency of des(Arg(141α)-HbA appears at 220 cm^{-1} as a single band, whereas two sublines at 201 cm^{-1} and 212 cm^{-1} were assigned to the α-subunit of HbA. In view of these findings, the sublines at 203 cm^{-1} and 212 cm^{-1} can be assigned to the α-subunit whereas in the β-subunits the sublines appear at 220 cm^{-1} and 227 cm^{-1}.

There are some discrepancies, however, concerning the heterogenity of the $\nu_{Fe\text{-}His}$ band. Whereas we found four sublines for the subunits in deoxyHbA the analysis of Ondrias et al. (1982) yields only three, i.e., two α-sublines and one single band for the β-chain. Furthermore the authors assigned the frequencies occuring at 218 cm^{-1} (α-subunit) and 222 cm^{-1} (β-subunit) of the des(Arg141α)-HbA spectrum exclusively to the *R*-state. Our results, however, suggest, that the corresponding sublines exist also in the *T*-state. Further experiments carried out with high spectral resolution are required to clarify whether the band profiles of the hybrids can also be decomposed into sublines.

Conformational heterogenity and the concept of conformational substates

A large number of investigations dealing with structure and function of heme proteins, especially of myoglobin, have revealed the existence of conformational substrates (CS) within a defined tertiary state (Austin et al., 1975, Frauenfelder et al., 1979, Parak, 1987). Ansari et al. (1985) have proposed that the CS are arranged in a hierachy of several tiers. At physiological temperatures the proteins fluctuate among substates of all tiers. As the temperature is lowered, the CS of the different tiers freeze out subsequently. The CS^0 states of upper tier 0, for instance, freeze out at 180 K, when the protein is in a glycerol-water solvent (Ansari et al., 1987, Frauenfelder et al., 1988, Ormos et al., 1990).

Some structural aspects of the CS^0-conformations could be obtained from the analysis of the CO-stretching band of MbCO. Makinen et al. (1979) have found, that for sperm whale Mb, this band can be decomposed into three different sublines. This observation was confirmed by Caughey et al. (1981) for bovine heart Mb. By means of polarization experiments Ormos et al. (1988) related

each subline to a distinct tilt angle between the CO-bond and the heme normal. Each of these obtained heme-ligand conformations was interpreted as a substate of tier 0 (CS^0).

It is reasonable to assume that this notion also holds for the conformational heterogenity of the Fe^{2+}-His(F8) bond monitored by the different sublines into which the $\nu_{Fe\text{-}His}$ bands of deoxyHbA and deoxyHb-trout IV can be decomposed. In the light of the coupling model introduced above, this would imply that different tilt angles of the Fe^{2+}-His(F8)-bond (reflected by different frequencies of the $\nu_{Fe\text{-}His}$-line) must be assigned to different CS^0-conformations. One may further speculate whether the sub-sublines composing each subline in deoxyHb trout IV correspond to substates of tier CS^1 exhibiting different azimuthal angles of the Fe^{2+}-His(F8)-bond in differing protonation states of the corresponding conformation CS^0.

Finally, it should be mentioned that hole burning experiments on the near IR-760 nm band (band III) resulting from a A_{2u}(porphyrin) $\rightarrow$ $d_{xy}(Fe^{2+})$ charge transfer transition provide considerable evidence for the existence of different subconformations of the Fe^{2+}-N_ϵ(His F8)-bond (Campbell et al., 1987; Chavez et al. [1990]). Moreover, these subconformations seem to exhibit different rebinding kinetics for CO indicating that the heterogeneity of the iron-protein linkage is of functional importance.

In conclusion this study provides evidence that the $\nu_{Fe\text{-}His}$-band of both deoxyHb-trout IV and deoxyHbA can be decomposed into different sublines. This can be rationalized in terms of different conformational substates of the Fe^{2+}-N_ϵ(His F8)-linkage exhibiting different polar (tilt) angles Θ with the respect to the heme normal. In deoxyHb-trout IV the protonation of Bohr groups change the intensity of the sublines by altering the azimuthal angle ϕ of the Fe^{2+}-N_ϵ(His F8)-bond.

Further characterization of the thus derived substates requires highly resolved measurements of the $\nu_{Fe\text{-}His}$-band at cyrogenic temperatures. This project is currently underway in our laboratory.

APPENDIX A1

Calculation of the molar fractions of the subconformations using model I

To calculate the molar fractions of the subconformations $C^{ij}_{m,s}$ introduced in model I we used the equation:

$$X^{ij}_{m,s}(\mathrm{pH}) = \frac{\exp\{[(i+j)\mu^{H+} - G(m,i,j,S)]/RT\}}{Z_s}, \quad \text{(A1.1)}$$

where μ^{H+} is the chemical potential of the protons, R is the gas constant and T the absolute temperature. $G(m,i,j,S)$ is the free energy of the mth subconformation in the protonation state $[i,j]$ and is given by:

$$G(m,i,j,S) = RT\{\ln(K^{ij}_{1m,s}) + i\,\mathrm{pK}_1(m,s) + j\,\mathrm{pK}_2(m,s)\}, \quad \text{(A1.2)}$$

where $K^{ij}_{1m,s}$ is the equilibrium constant for the transition between the subconformations 1 and m in the protonation state $[i,j]$ ($K^{ij}_{11,s} = 1$). The pK-values of the two Bohr groups in the conformation m are denoted by $pK_1(m,s)$ and $pK_2(m,s)$, respectively. The grand partition sum Z is written as:

$$Z_s = \sum_m \sum_{ij} [\exp\{[(i+j)\mu^{H+} - G(m,i,j,S)]/RT\}]. \quad \text{(A1.3)}$$

APPENDIX A2

Calculation of the molar fractions of the titration states of a subunit S using model II

The mass action law was applied to calculate the molar fraction $X^{ij}_s(\mathrm{pH})$ of the protonation state C^{ij}_s:

$$\tilde{X}^{00}_s = \{1 + [H^+]/K_{1,s} + [H^+]/K_{2,s} + [H^+]^2/(K_{1,s}K_{2,s})^{-1}\} \quad \text{(A2.1}a\text{)}$$

$$\tilde{X}^{10}_s = \{1 + K_{1,s}/[H^+] + [H^+]/K_{2,s} + K_{1,s}/K_{2,s}\}^{-1} \quad \text{(A2.1}b\text{)}$$

$$\tilde{X}^{01}_s = \{1 + [H^+]/K_{1,s} + K_{2,s}/[H^+] + K_{2,s}/K_{1,s}\}^{-1} \quad \text{(A2.1}c\text{)}$$

$$\tilde{X}^{11}_s = \{1 + K_{1,s}/[H^+] + K_{2,s}/[H^+] + K_{1,s}K_{2,s}/[H^+]^2\}^{-1}. \quad \text{(A2.1}d\text{)}$$

We would to like thank Mr. Gerd Ankele for technical assistance. Dipl. Phys. Andreas Stichternath wrote the computer program used for the line shape analysis. On recommendation of one referee Diplom-Physiker Harald Gilch measured the $\nu_{Fe\text{-}His}$-band with different laser power.

The work was supported by a grant from the Deutsche Forschungsgemeinschaft.

Received for publication 2 January 1991 and in final form 2 April 1991.

REFERENCES

Ansari, A., J. Berendzen, S. F. Bowne, H. Frauenfelder, I. E. T. Iben, T. B. Sauke, E. Shysamunder, and R. D. Young. 1985. Protein states and protein quakes. *Proc. Natl. Acad. Sci. USA.* 85:5000–5004.

Ansari, A., J. Berendzen, D. Braunstein, B. R. Cowen, H. Frauenfelder, M. K. Hong, I. E. T. Iben, J. B. Johnson, P. Ormos, T. B. Sauke, R. Scholl, A. Schulte, P. J. Steinbach, R. D. Vittitow, and R. D. Young. 1987. Rebinding and relaxation in the myoglobin pocket. *Biophys. Chem.* 26:337–335.

Bangcharoenpaurpong, O., K. T. Schomaker, and P. M. Champion. 1984. A resonance Raman investigation of myoglobin. *J. Am. Chem. Soc.* 106:5688–5698.

Baldwin, J. L., and C. Chothia. 1979. Haemoglobin, the structural changes related to ligand binding and its allosteric mechanism. *J. Mol. Biol.* 129:175–200.

Brunori, M. 1975. Molecular adaptation to physiological requirements: the hemoglobin system of trout. *Curr. Top. Cell Regul.* 9:1–39

Brunori, M., M. Coletta, B. Giardina, and J. Wyman. 1978. A macromolecular transducer as illustrated by hemoglobin trout IV. *Proc. Natl. Acad. Sci. USA.* 75:4310–4312.

Campbell, B. F., M. R. Chance, and J. M. Friedman. 1987. Linkage of functional and structural heterogenity in proteins: dynamic hole burning in carboxymyoglobin. *Science (Wash. DC).* 238:373–376.

Caughey, W. S., H. Shimada, M. G. Choc, and M. P. Tucker. 1981. Dynamic protein structures: infrared evidence for four discrete rapidly interconverting conformers at the carbon monoxide binding site of bovine heart myoglobin. *Proc. Natl. Acad. Sci. USA.* 78:2903–2907.

Chavez, M. D., S. H. Courtney, M. R. Chance, D. Kiula, J. Nocek, B. M. Hofmann, J. Friedman, and M. R. Ondrias. 1990. Structural and functional significance of inhomogenous line broadening of band III in hemoglobin and Fe-Mn hybrid hemoglobin. *Biochemistry.* 29:4844–4852

Chien, J. C. W., and K. H. Mayo. Carp hemoglobin. I. Precise oxygen equilibrium and analysis according to the models of Adair and of Monod, Wyman, and Changeux. 1980. *J. Biol. Chem.* 255:9790–9799.

Frauenfelder, H., G. A. Petsko, and D. Tsernoglou. 1979. Temperature dependent x-ray diffraction as a probe of protein structural dynamics. *Nature (Lond.).* 280:558–563.

Frauenfelder, H., F. Parak, and R. D. Young. 1988. Conformational substates in proteins. *Annu. Rev. Biophys. Biophys. Biochem.* 17:451–479.

Friedman, J. M., T. W. Scott, R. A. Stepnoski, M. Ikedo-Saito, and T. Yonetari. 1983. The iron-proximal histidine linkage and protein control of oxygen binding in hemoglobin. *J. Biol. Chem.* 10:10564–10572.

Friedman, J. M. 1985. Structure, dynamics and reactivity in hemoglobin. *Science (Wash. DC).* 228:1274–1280.

Friedman, J. M., and D. L. Rousseau. 1988. Transient and cyrogenic studies of photodissociated hemoglobin and myoglobin. *In* Biological Application of Raman Spectroscopy. T. G. Spiro, editor. 133–216.

Friedman, J. M., B. F. Campbell, and R. W. Noble. 1990. A possible new control mechanism suggested by resonance Raman spectra from a deep ocean fish hemoglobin. *Biophys. Chem.* 37:43–59.

Herzfeld, J., and E. Stanley. 1974. A general approach to cooperativity and its application to the oxygen equilibrium of hemoglobin and its effectors. *J. Mol. Biol.* 82:231–265.

Kitagawa, T. 1988. Heme protein structure and the iron histidine stretching mode. *In* Biological Application of Raman Spectroscopy. T. G. Spiro, editor. 97–132.

Makinen, M. W., R. A. Houtchens, and W. S. Caughey. 1979. Structure of carboxymyoglobin in crystals and in solution. *Proc. Natl. Acad. Sci. USA.* 76:6042–6046.

Matsukawa, S., K. Mawatari, Y. Yoneyama, and T. Kitagawa, 1985. Correlation between iron-histidine stretching frequencies and oxygen affinity of hemoglobins. A continuous strain model. *J. Am. Chem. Soc.* 107:1108–1116.

Nagai, K., and T. Kitagawa. 1980. Difference in Fe(II)-N_ϵ (His-F8) stretching frequencies between deoxyhemoglobins in the two alternative quaternary structures. *Proc. Natl. Acad. Sci. USA. 77:2033–2037.*

Nagai, K., T. Kitagawa, and H. Morimoto. 1980. Quaternary structures and low frequency molecular vibrations of haems of deoxy and oxyhaemoglobin studied by resonance Raman scattering. *J. Mol. Biol.* 136:271–289.

Noble, R. W., L. J. Parkhurst, and Q. H. Gibson. 1970. The effect of pH on the reactions of oxygen and carbon monoxide with the hemoglobin of the carp. *J. Biol. Chem.* 245:6628–6633.

Parak, F. 1987. A model of protein dynamics inferred from x-ray structure analysis and Mössbauer spectroscopy on myoglobin. *Mol. Cell. Biophys.* 4:265–280.

Perkampus, H. H. 1986. UV-Vis-Spectroskopie und ihre Anwendung. Springer Verlag, Berlin.

Perutz, M. F. 1970*a*. Stereochemistry of cooperative effects in haemoglobin. *Nature (Lond.).* 228:726–734.

Perutz, M. F. 1970*b*. The Bohr effect and combination with organic phosphates. *Nature (Lond.).* 228:734–739.

Perutz, M. F., and M. Brunori. 1982. Stereochemistry of cooperative effects in fish and amphibian hemoglobin. *Nature (Lond.).* 299:421–426.

Ondrias, M. R., D. L. Rousseau, T. Kitagawa, M. Ikeda-Saito, T. Inubushi, and T. Yonetani. 1982. Quaternary structure changes in iron-cobalt hybrid hemoglobins detected by resonance Raman scattering. *J. Biol. Chem.* 10:8766–8770.

Ormos, P. D., D. Braunstein, H. Frauenfelder, M. K. Hong, S.-L. Lin, T. B. Sauke, and R. D. Young. 1988. Orientation of carbon monoxide and structure-function relationship in carbonmonoxymyoglobin. *Proc. Natl. Acad. Sci. USA.* 85:8492–8496.

Ormos, P., A. Ansari, D. Braunstein, B. R. Cowen, H. Frauenfelder, M. K. Hong, I. E. T. Iben, T. B. Sauke, P. J. Steinbach, and R. D. Young. 1990. Inhomogenous broadening in spectral bands of carbonmonoxymyoglobin. The connection between spectral and functional heterogenity. *Biophys. J.* 57:191–200.

Sassaroli, M., S. Dasgupta, and D. L. Rousseau. 1986. Cryogenic stabilization of myoglobin photoproducts. *J. Biol. Chem.* 261:13704–13713.

Scheidt, W. R., and D. M. Chipman. 1986. Preferred orientation of Imidazole, ligands in metallophorphyrins. *J. Am. Chem. Soc.* 108: 1163–1167.

Schweitzer-Stenner, R., W. Dreybrodt, and S. el Naggar. 1984. Investigation of pH-induced symmetry distortions of the prosthetic group in deoxyhaemoglobin by resonance Raman scattering. *Biophys. Struct. Mech.* 10:241–256.

Schweitzer-Stenner, R., D. Wedekind, and W. Dreybrodt. 1986. Correspondence of the pK-values of oxy-Hb titration states detected by resonance Raman scattering to kinetic data of ligand association and dissociation. *Biophys. J.* 49:1077–1088.

Schweitzer-Stenner, R., and W. Dreybrodt. 1989. An extended Monod-Wyman-Changeaux model expressed in terms of the Herzfeld-Stanley formalism applied to oxygen and carbon monoxide binding curves of hemoglobin trout IV. *Biophys. J.* 55:691–701.

Schweitzer-Stenner, R., D. Wedekind, and W. Dreybrodt. 1989*a*. Detection of heme perturbations caused by the quaternary R → T transition in oxyhemoglobin trout IV by Resonance Raman scattering. *Biophys. J.* 55:703–712.

Schweitzer-Stenner, R., D. Wedekind and W. Dreybrodt. 1989*b*. The influence of structural variations in the F- and FG-helix of the β-subunit modified oxyHb-NES on the heme structure detected by resonance Raman spectroscopy. *Eur. Biophys. J.* 17:87–100.

Schweitzer-Stenner, R. 1989. Allosteric linkage induced distortions of the prosthetic group in haem proteins as derived by the theoretical interpretation of the depolarization ratio in Resonance Raman scattering. *Quart. Rev. Biophys.* 22:381–497.

Shaanan, B. 1983. Structure of human oxyhemoglobin at 2.1 Å resolution. *J. Mol. Biol.* 171:31–59.

Spiro, T. G., and T. C. Strekas. 1974. Resonance Raman spectra of heme proteins: effects of oxidation and spin state. *J. Am. Chem. Soc.* 96:337–345.